

LETTER TO THE EDITOR

The angular momentum-mass relation: a fundamental law from dwarf irregulars to massive spirals

Lorenzo Posti^{1,*}, Filippo Fraternali¹, Enrico M. Di Teodoro² and Gabriele Pezzulli³

¹ Kapteyn Astronomical Institute, University of Groningen, P.O. Box 800, 9700 AV Groningen, the Netherlands

² Research School of Astronomy and Astrophysics - The Australian National University, Canberra, ACT, 2611, Australia

³ Department of Physics, ETH Zurich, Wolfgang-Pauli-Strasse 27, 8093 Zurich, Switzerland

Received XXX; accepted YYY

ABSTRACT

In a Λ CDM Universe, the specific stellar angular momentum (j_*) and stellar mass (M_*) of a galaxy are correlated as a consequence of the scaling existing for dark matter haloes ($j_h \propto M_h^{2/3}$). The shape of this law is crucial to test galaxy formation models, which are currently discrepant especially at the lowest masses, allowing to constrain fundamental parameters, e.g. the retained fraction of angular momentum. In this study, we accurately determine the empirical $j_* - M_*$ relation (Fall relation) for 92 nearby spiral galaxies (from S0 to Irr) selected from the *Spitzer* Photometry and Accurate Rotation Curves (SPARC) sample in the unprecedented mass range $7 \lesssim \log M_*/M_\odot \lesssim 11.5$. We significantly improve all previous estimates of the Fall relation by determining j_* profiles homogeneously for all galaxies, using extended HI rotation curves, and selecting only galaxies for which a robust j_* could be measured (converged $j_*(<R)$ radial profile). We find the relation to be well described by a single, unbroken power-law $j_* \propto M_*^\alpha$ over the entire mass range, with $\alpha = 0.55 \pm 0.02$ and orthogonal intrinsic scatter of 0.17 ± 0.01 dex. We finally discuss some implications for galaxy formation models of this fundamental scaling law and, in particular, the fact that it excludes models in which discs of all masses retain the same fraction of the halo angular momentum.

Key words. galaxies: kinematics and dynamics – galaxies: spiral – galaxies: structure – galaxies: formation

1. Introduction

Mass (M) and specific angular momentum ($j = J/M$) are two independent and key galaxy properties, subject to physical conservation laws, which are correlated in a fundamental scaling relation, the $j_* - M_*$ law. This was first introduced by Fall (1983), as a basis for a physically-motivated classification of galaxies, and hence we call it the *Fall relation* hereafter. Empirically, massive spiral galaxies ($\log M_*/M_\odot \gtrsim 9$) are found to lie on a power-law relation close to $j_* \propto M_*^{2/3}$ (Romanowsky & Fall 2012, hereafter RF12).

In a Λ Cold Dark Matter (Λ CDM) Universe, this fundamental relation highlights the intimate link between galaxies and their host dark matter haloes: in fact, the specific angular momentum of haloes scales precisely as their mass to the power 2/3, as a result of tidal torques (Peebles 1969; Efstathiou & Jones 1979). As highlighted by early semi-analytic models (Dalcanton, Spergel, & Summers 1997; Mo, Mao, & White 1998), this connection is mediated by two fundamental physical parameters: $f_{M,*} \equiv M_*/M_h$, the so-called *global star-formation efficiency*, and $f_{j,*} \equiv j_*/j_h$, the so-called *retained fraction of angular momentum*, which encapsulates several processes relevant to galaxy formation, including angular momentum losses due to interactions and the possibility that the gas which contributes to star formation does not sample uniformly the global angular momentum distribution. In particular, the observed Fall relation is key to constrain $f_{j,*}$ as a function of other galaxy properties (Posti et al. 2018; Shi et al. 2017).

Several galaxy formation models are now able to correctly predict the amount of angular momentum in massive spiral galaxies (e.g. Genel et al. 2015; Teklu et al. 2015; Zavala et al. 2016). However, these predictions become rather discrepant and uncertain for the lower mass systems ($\log M_*/M_\odot \lesssim 9$), where some models predict a flattening of the relation (Obreja et al. 2016; Stevens, Croton, & Mutch 2016; Mitchell et al. 2018) while others do not see any change with respect to the relation for larger spirals (El-Badry et al. 2018). These discrepancies are arising also because observational estimates of the $j_* - M_*$ relation over a wide galaxy stellar-mass range are lacking.

The aim of the present Letter is to provide the benchmark for the Fall relation from dwarf to massive spirals in the local Universe. We use spirals of all morphological types spanning an unprecedented mass range ($7 \lesssim \log M_*/M_\odot \lesssim 11.5$), using accurate near-infrared photometry/HI data to trace the stellar mass/galaxy rotation out to several effective radii. Unlike many previous estimates of massive (RF12; Obreschkow & Glazebrook 2014; Cortese et al. 2016) and dwarfs separately (Butler, Obreschkow, & Oh 2017; Chowdhury & Chhengalur 2017), we homogeneously measure j_* profiles for all galaxies and determine the relation using only those with a converged value of the total j_* .

The paper is organised as follows. Sect. 2 introduces the dataset used. Sect. 3 explains our method and selection criteria and presents our determination of the Fall relation. In Sect. 4 we discuss the implications of our findings for galaxy formation models. We summarize and conclude in Sect. 5.

* posti@astro.rug.nl

2. Data

The sample of spiral and irregular galaxies considered in this work comes from the *Spitzer* Photometry and Accurate Rotation Curves (SPARC) sample (Lelli, McGaugh, & Schombert 2016b, hereafter LMS16). For these 175 nearby galaxies, from S0 to Irr, surface brightness profiles at $3.6\ \mu\text{m}$, derived from *Spitzer* Space Telescope photometry, and high-quality neutral hydrogen (HI) rotation curves, derived from interferometric HI data, are available.

Near-infrared profiles best trace the stellar mass distribution (e.g. Verheijen 2001), as the mass-to-light ratio at $3.6\ \mu\text{m}$ is nearly constant over a broad range of galaxy masses and morphologies (e.g. Bell & de Jong 2001; McGaugh & Schombert 2014). For this work we assume the fiducial values used in Lelli et al. (2017) for stellar population models with a Chabrier (2003) initial mass function: $\Upsilon_b^{[3.6]} = 0.5$ and $\Upsilon_d^{[3.6]} = 0.7$ for the bulge and disc at $3.6\ \mu\text{m}$, respectively¹. The photometric profiles have also been decomposed in bulge/disc as described in LMS16.

In a disc galaxy most stars are on nearly-circular orbits and rotate with velocities close to the local circular speed. We use the available HI rotation curves (from LMS16) to trace the circular velocity, then we apply a correction for the asymmetric drift (Binney & Tremaine 2008, §4.8.2) to get the stellar rotation curve (see Sect. A).

3. The specific angular momentum-mass relation

If a galaxy is axisymmetric and rotates on cylinders about its symmetry axis, then the *specific stellar angular momentum* $j_* \equiv |\mathbf{J}_*|/M_*$ within the radius R from the galactic centre writes as

$$j_*(< R) = \frac{\int_0^R dR' R'^2 \Sigma_*(R') V_{*,\text{rot}}(R')}{\int_0^R dR' R' \Sigma_*(R')}, \quad (1)$$

where $\Sigma_*(R) = \Upsilon_b^{[3.6]} I_b(R) + \Upsilon_d^{[3.6]} I_d(R)$ is the surface stellar mass density, with I_b and I_d being the surface brightnesses of the bulge/disc at $3.6\ \mu\text{m}$, and $V_{*,\text{rot}}$ the stellar rotation curve. The total specific stellar angular momentum is $j_* \equiv j_*(< R_{\text{max}})$, where R_{max} is the outermost radius at which Σ_* is measured. We compute the galaxy stellar mass as $M_* = 2\pi \int_0^{R_{\text{max}}} dR' R' \Sigma_*(R')$.

3.1. Specific angular momentum profiles and sample selection

We use Eq. 1 to compute the specific angular momentum as a function of radius. We plot the resulting $j_*(< R)$ profiles for all the galaxies in the SPARC sample in Figure 1. We find that for most galaxies $j_*(< R)$ rises steeply in the inner parts and then flattens at about $\sim 5R_d$. The profiles typically flatten close to the value of the specific angular momentum of a thin exponential disc (with scale length R_d) with a constant rotation curve V_f , i.e. $j_{*,\text{exp}} = 2R_d V_f$. As expected, most of the specific angular momentum of a spiral galaxy resides further out its optical half-light radius and radially extended rotation curves, such as those provided by HI observations, are *crucial* to properly measure it.

¹ These values are comparable with those used by Fall & Romanowsky (2013) in their updated calibration of the Fall relation with respect to RF12, who used $\Upsilon^K = 1$ (in K -band) for both bulge and disc.

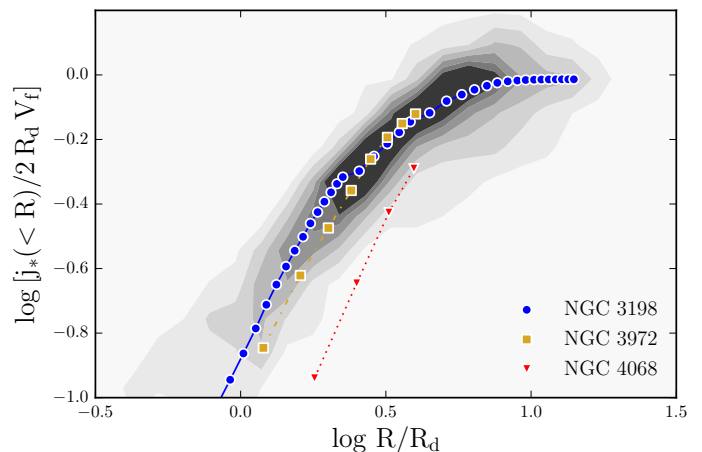


Fig. 1. Stellar specific angular momentum profiles for 175 disc galaxies in the SPARC sample. Grey contours represent the distribution of all the points in the profile of each galaxy. The radius is normalised to the disc scale length (R_d at $3.6\ \mu\text{m}$) and j_* to that of a thin exponential disc with the same R_d and with a constant rotation curve. We also show the full profiles for three representative galaxies in our initial sample: a galaxy with a fully converged $j_*(< R)$ profile (blue circles), a galaxy with a converging profile (yellow squares) and a galaxy with a non-converging profile (red triangles). For our determination of the Fall relation, we excluded galaxies with a non-converging profile.

In fact, all the galaxies with extended rotation curves have fully-converged j_* profiles, while only lower limits on j_* can be determined for some galaxies for which the rotation curve at large radii is not known.

The value $j_{*,\text{exp}} = 2R_d V_f$ has been used by several authors as an estimate of the specific angular momentum for disc galaxies (Fall 1983, RF12). However, the actual $j_*(< R)$ of spirals flattens at about $j_{*,\text{exp}}$ with a significant scatter (~ 0.12 dex at $\sim 5R_d$), hence we caution against using simple estimates of the specific angular momentum.

To determine robustly the Fall relation for local spirals, we use only galaxies with an accurate measurement of j_* , i.e. only those with a converging $j_*(< R)$ profile. Thus, being R_0, \dots, R_N the radii at which the j_* profiles are sampled, we select galaxies satisfying the following criteria:

$$\frac{j_*(< R_N) - j_*(< R_{N-1})}{j_*(< R_N)} < 0.1 \quad \& \quad \left. \frac{d \log j_*(< R)}{d \log R} \right|_{R_N} < \frac{1}{2}, \quad (2)$$

i.e. that the last two points of the j_* profile differ by less than 10% and that the logarithmic slope of the j_* profile in the outermost point is less than $1/2$.

To further illustrate our selection, we highlight in Fig. 1 the individual j_* profiles of three galaxies in the SPARC sample, representative of different converging properties. NGC 3198 has a perfectly converged j_* profile (blue circles). In our sample, 28 galaxies, covering the entire SPARC mass range, show a similar feature: these are the galaxies for which j_* is best measured. NGC 3972 (yellow squares) is the archetype of the galaxies that merely comply to the criteria of Eq. 2; these galaxies have a converging j_* profile and the difference between the last two points of the profile is smaller than 10%. NGC 4068 (red triangles) has a steeply rising j_* profile that does not meet Eq. 2 criteria; 34 similar galaxies are excluded from the calibration of the local Fall relation since their total j_* might be severely underestimated.

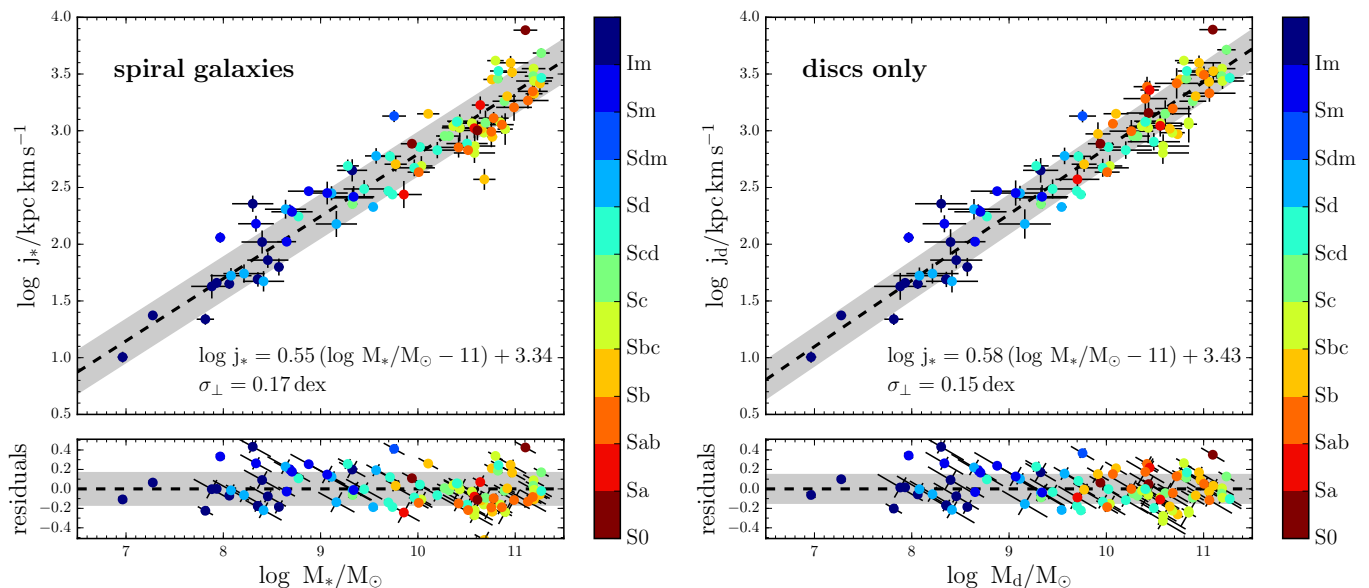


Fig. 2. *Left-hand panel:* specific stellar angular momentum-stellar mass relation (Fall relation) for a sample of 92 nearby disc galaxy. Each galaxy is represented by a circle coloured by Hubble type. The black dashed line is the best-fitting linear model and the grey band is the 1σ orthogonal intrinsic scatter. The bottom panel shows the orthogonal residuals around the linear model. *Right-hand panel:* same as the left-hand panel, but for the discs only (i.e. after removing the contribution from the bulges).

We finally excluded galaxies with inclination angles below 30° , as their rotation velocity is very uncertain, and we are left with a sample of 92 galaxies with masses $7 \lesssim \log M_*/M_\odot \lesssim 11.5$. For those, we estimate the uncertainty in the stellar mass following Lelli, McGaugh, & Schombert (2016a, see their Section 2.3) and the error on j_* as

$$\delta_{j_*} = R_d \sqrt{\frac{1}{N} \sum_i \delta_{v_i}^2 + \left(\frac{V_f}{\tan i} \delta_i\right)^2 + \left(V_f \frac{\delta_D}{D}\right)^2}, \quad (3)$$

where V_f is the velocity in the flat part of the rotation curve (see Lelli, McGaugh, & Schombert 2016a), i is the inclination and δ_i its uncertainty, D is the distance and δ_D its uncertainty and δ_{v_i} is the uncertainty at each point in the rotation curve. The error on distance often dominates the error budget. Of the 92 galaxies selected, 49 (53%) have relatively uncertain distances estimated with the Hubble flow (with relative errors of 10 – 30%), while 43 (47%) have distances known within better than 10% (mostly from red giant branch tip).

3.2. The $j_* - M_*$ relation for galaxies and their discs

The left-hand panel of Figure 2 shows our determination of the specific angular momentum-mass relation for nearby disc galaxies over ~ 5 dex in stellar mass. We fit a linear relation (in logarithm) to the data points allowing for an *orthogonal* intrinsic² scatter. We assume uninformative priors for the three parameters (slope, normalisation and scatter) and explore the posterior distribution with a Monte Carlo Markov Chain (MCMC) method (using the python implementation by Foreman-Mackey et al. 2013). With a model that follows

$$\log j_* = \alpha [\log(M_*/M_\odot) - 11] + \beta, \quad (4)$$

² We subtract the contribution to the total scatter from measurement uncertainties.

we find a best-fitting slope $\alpha = 0.55 \pm 0.02$, a normalisation $\beta = 3.34 \pm 0.03$ and an orthogonal intrinsic scatter $\sigma_\perp = 0.17 \pm 0.01$ dex. We repeated this exercise i) varying the thresholds in Eq. 2 and ii) considering only the 20 galaxies with converged j_* profiles that have distances known better than 10%, and found no significant difference in the best-fit relation. In these estimates we have assumed the uncertainties in M_* and j_* to be uncorrelated; however, this is likely not the case since both δ_{M_*} and δ_{j_*} are often dominated by distance errors. Hence, we recomputed again the distributions of the model parameters in the extreme case of fully correlated uncertainties (correlation coefficient unity): we find no significant difference in neither the slope nor the normalisation, but we find a slightly larger orthogonal intrinsic scatter $\sigma_\perp = 0.179 \pm 0.014$ dex.

The best-fitting values are consistent, albeit having a smaller intrinsic scatter, with previous estimates of the Fall relation for high-mass spirals. We also confirm that the residuals correlate with galaxy morphology: earlier galaxy types are found systematically below the relation and viceversa for later types (RF12; Cortese et al. 2016). While significantly improving the determination of the relation at high masses³, we have robustly measured that the Fall relation extends to dwarf galaxies as a single, unbroken power-law. This is a crucial observational result that challenges many state-of-the-art galaxy formation models, which predict a flattening of the relation at low masses (Stevens, Croton, & Mutch 2016; Obreja et al. 2016; Mitchell et al. 2018).

We note that two previous works looked at the *baryonic* version of the specific angular momentum-mass law for dwarf irregulars and found them to be offset towards larger j_{baryon} with respect to the relation for massive spirals (Butler, Obreschkow, & Oh 2017; Chowdhury & Chengalur 2017). Our rotation curves (from the SPARC sample) have been specifically selected to be of the highest possible quality and hence to better trace the axisymmetric gravitational potential. We are planning to use this

³ RF12 used the simple $j_{*,\text{exp}}$ estimator, Cortese et al. (2016) computed j_* only within the optical effective radius and Obreschkow & Glazebrook (2014) had only 16 objects.

Table 1. Best-fit parameters, and their 1σ errors, of the function $\log j = \alpha(\log M - 11) + \beta$ fitted to the data in Fig. 2 for galaxies and their discs. σ_{\perp} is the orthogonal intrinsic scatter.

	α	β	σ_{\perp}
Spiral galaxies	0.55 ± 0.02	3.34 ± 0.03	0.17 ± 0.01
Discs only	0.585 ± 0.020	3.43 ± 0.03	0.15 ± 0.01

dataset to investigate the baryonic relation in a forthcoming paper. Butler, Obreschcow, & Oh (2017) also showed a $j_* - M_*$ relation down to low-mass galaxies which is offset towards larger j_* and much more scattered than ours. This is most likely due to i) the different quality of their rotation curves (see e.g. Iorio et al. 2017, their Fig. 24) and ii) to their use of fitting functions to extrapolate the total j_* as opposed to our check of its convergence on each individual galaxy. Moreover, we have checked our results against a different determination of the circular velocities for a sample of 17 dwarf irregulars by Iorio et al. (2017), who used the state-of-the-art 3D software 3D-BAROLO (Di Teodoro & Fraternali 2015). We found that the j_* profiles of the galaxies in common with SPARC are consistent.

The Fall relation in the left-hand panel of Fig. 2 is amongst the tightest known scaling laws for spiral galaxies⁴. However, the relation gets even tighter if one considers just the disc component of spiral galaxies, i.e. by removing the bulge contribution to the light profile. The right-hand panel of Fig. 2 shows the disc specific angular momentum-mass relation ($j_d - M_d$) and Table 1 summarises the results for both the $j_* - M_*$ and $j_d - M_d$ relation. We find that the relation for discs has the following important differences with respect to the one for whole stellar body:

- S0-Sb galaxies with $\log M_*/M_{\odot} \gtrsim 9.5$ scatter around null residuals in the $j_d - M_d$ relation. This significantly alleviates the trend of the residuals with galaxy morphology, present in the $j_* - M_*$ relation;
- the scatter of the $j_d - M_d$ relation, $\sigma_{\perp} = 0.15 \pm 0.01$ dex, is slightly smaller and its slope, $\alpha = 0.585 \pm 0.020$, is slightly larger than that of the $j_* - M_*$ relation.

These two points are particularly important because they suggest that the $j_d - M_d$ is more fundamental than the $j_* - M_*$ relation. In particular, the best-fit slope of the relation for discs is closer to that of dark matter haloes, $j_h \propto M_h^{2/3}$, possibly indicating a simpler link to dark haloes of discs compared to bulges (e.g. Mo, Mao, & White 1998). In the next Section we discuss some implications of the $j_d - M_d$ relation for galaxy formation models.

4. Physical models

In a Λ CDM cosmology, dark matter haloes acquire angular momentum from tidal torques such that their specific angular momentum $j_h \propto \lambda M_h^{2/3}$, being M_h their (virial) mass and λ the so-called dimensionless spin parameter (which is independent from mass, see Peebles 1969). It follows that discs, which form inside these haloes out of gas that has initially the same initial angular momentum as the dark matter, will have specific angular momentum

$$j_d \propto \lambda f_{j,d} f_{M,d}^{-2/3} M_d^{2/3}, \quad (5)$$

where we have defined the stellar disc’s “global star-formation efficiency” $f_{M,d} \equiv M_d/M_h$ and the stellar disc’s “retained fraction

⁴ For comparison the baryonic Tully-Fisher relation has an intrinsic orthogonal scatter of about $\sim 0.07 - 0.05$ dex (Ponomareva et al. 2018).

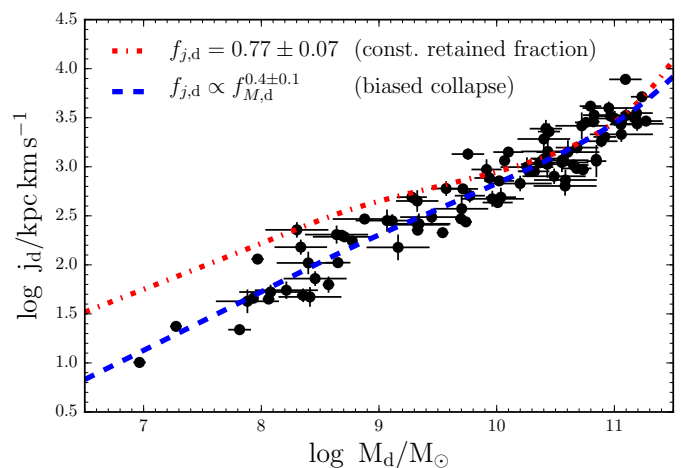


Fig. 3. Predicted distribution in the $j_d - M_d$ plane of a model with a constant retained fraction of angular momentum f_j (red dot-dashed line) and for a *biased collapse* model (blue dashed line) compared to the data as in Fig. 2. To compute the two models we have used the stellar-to-halo mass relation from Rodríguez-Puebla et al. (2015).

of angular momentum” $f_{j,d} \equiv j_d/j_h$ (e.g. Posti et al. 2018). In what follows we will use the recent estimate of the stellar-to-halo mass relation for late-type galaxies by Rodríguez-Puebla et al. (2015) as our fiducial $f_{M,d}$ (see Posti et al. 2018, for other choices).

We first consider the case in which all spirals retain the same fraction of the halo’s angular momentum (e.g. Mo, Mao, & White 1998). This case is of particular interest since several state-of-the-art semi-analytic galaxy formation models are based on the assumption of a constant $f_{j,d}$ for all masses (see e.g. Knebe et al. 2015, for a comparison of many of these). In this case, Eq. 5 reduces to $j_d \propto f_{M,d}^{-2/3} M_d^{2/3} = M_h^{2/3}$, which we show in Figure 3 in comparison with the data (red dot-dashed line). We fitted this model for the value of the constant retained fraction and we found it significantly smaller than unity, $f_{j,d} = 0.77 \pm 0.7$ (similar to previous findings, e.g. Dutton & van den Bosch 2012, RF12). While the model provides a decent fit to the data for high-mass discs ($\log M_*/M_{\odot} \sim 10.5$), indicating that about 70 – 80% of the halo’s angular momentum is incorporated in these galaxies, the model also clearly over-predicts j_d in low-mass galaxies ($\log M_*/M_{\odot} \lesssim 9$), which instead require a much smaller $f_{j,d}$ (see also Figure 1 in Posti et al. 2018).

Some semi-analytic galaxy formation models (Knebe et al. 2015; Stevens, Croton, & Mutch 2016) as well as some others based on numerical hydrodynamical simulations (Genel et al. 2015; Obreja et al. 2016; Mitchell et al. 2018) do show similar predictions of a flattening of the Fall relation at $M_* \sim 10^9 M_{\odot}$, which are inconsistent with our accurate determination of the $j_* - M_*$ law. This is, in fact, related to the retained fraction of angular momentum $f_{j,d}$ which they either assume or find to be relatively constant as a function of galaxy mass. In other models, instead, strong stellar feedback is crucial to make low-mass discs have a lower $f_{j,d}$ – which also decreases to smaller masses – and are in fact able to predict qualitatively well the Fall relation in the full mass range that we probe observationally (El-Badry et al. 2018).

The last physical models that we consider in this discussion are inside-out cooling models in which star-formation proceeds from angular momentum-poor to angular momentum-rich gas: the so-called *biased collapse* models (Dutton & van den Bosch

2012; Kassin et al. 2012, RF12). Following Posti et al. (2018), if for the gas, as for the dark matter, the angular momentum is distributed as $j(< R) \propto M(< R)^s$, with s being a constant slope (see Bullock et al. 2001), then $f_{j,d} \propto f_{M,d}^s$ (van den Bosch 1998; Navarro & Steinmetz 2000). Plugged into Eq. 5, this yields $j_d \propto f_d^{s-2/3} M_d^{2/3}$. We fit this prediction for the best value of s , which we find to be $s = 0.4 \pm 0.1$, and we show how that compares to the observed Fall relation in Fig. 3 (blue dashed line). This model provides a remarkable fit to the observations over the entire mass range and it is preferred to the constant- $f_{j,d}$ one (according to the Bayesian Information Criterion). The slope s in this model is related to the canonical angular momentum distribution $dM/dj \propto j^q$ where $s = 1/(1+q)$ and, perhaps unsurprisingly, its best-fitting value is compatible with that expected for pure discs ($q \approx 1$ in the low- j regime, van den Bosch, Burkert & Swaters 2001).

Finally we note that the scatter that we measure for the Fall relation ($\sigma_{\perp} = 0.15$ dex) is significantly smaller than what one might expect from Eq. (5), given that the scatter in the λ distribution is ~ 0.25 dex and that in the stellar-to-halo mass relation is ~ 0.15 dex. This suggests that i) the scatters of the $\lambda - M_h$, $f_{j,d} - M_h$ and $M_d - M_h$ relations are correlated such that when combined in Eq. (5) they yield the observed scatter and/or ii) the λ distribution of haloes hosting spiral galaxies is intrinsically narrower than that of the full halo population (even if the latter can not alone explain the measured specific angular momenta of massive spirals and ellipticals, see Posti et al. 2018).

5. Summary & Conclusions

In this Letter we have studied the relation between specific angular momentum and mass (Fall relation) of nearby disc galaxies spanning an unprecedented range in stellar mass ($7 \lesssim \log M_*/M_{\odot} \lesssim 11.5$). We have used *Spitzer* 3.6 μm photometry and HI rotation curves, compiled in the SPARC sample, to trace respectively the stellar mass surface density and rotation velocity profiles. We determine specific angular momentum profiles for all galaxies and use only those with converging profiles in the determination of the scaling law, since they guarantee an accurate measurement of the total galactic angular momentum. We find that:

- (i) the Fall relation, $j_* - M_*$ is remarkably well represented by a single power-law, with slope $\alpha = 0.55 \pm 0.02$ and scatter $\sigma_{\perp} = 0.17 \pm 0.01$ dex, from massive to dwarf spiral galaxies;
- (ii) the disc-only relation $j_d - M_d$ has a slightly steeper slope $\alpha = 0.585 \pm 0.020$ and a slightly smaller scatter $\sigma_{\perp} = 0.15 \pm 0.01$ dex;
- (iii) the observed Fall relation is a powerful benchmark for galaxy formation scenarios and poses a challenge to some of the current models, which predict a change of slope at low masses.

Being a scaling law that tightly relates two fundamental and independent quantities subject to physical conservation laws, the Fall relation stands out as one of the most (if not *the* most fundamental scaling relation for disc galaxies. From dwarf irregulars to massive spirals, from early-types (S0) to late-type spirals (Sd-Sm), all disc galaxies in the local Universe appear to lie on a single power-law relation, which may already be in place in the early Universe (Burkert et al. 2016; Harrison et al. 2017).

We also discussed how these remarkable observations can be used to constrain galaxy formation models. In particular, the Fall relation uniquely constrains how much of the angular momentum initially present in the baryons ends up being encapsulated

in the stellar body of a galaxy. Models assuming this to be a constant with galaxy mass will inevitably fail at reproducing the observations.

Among those considered, an inside-out cooling model (biased collapse) works better in reproducing the observed law. This scenario also points to some angular momentum redistribution taking place during star formation, possibly due to feedback, or to significant differences between the angular momenta of dark matter and baryons at start. Understanding the precise nature of these processes and in general giving account of the observed straight and tight $j_* - M_*$ relation across almost 5 orders of magnitude in stellar mass is a key challenge of modern theoretical astrophysics.

References

- Binney J., Tremaine S., 2008, *Galactic Dynamics*: 2nd edn. (Princeton University Press)
- Bell E. F., de Jong R. S., 2001, *ApJ*, 550, 212
- Brook C. B., Stinson G., Gibson B. K., Roškar R., Wadsley J., Quinn T., 2012, *MNRAS*, 419, 771
- Bullock J. S., Dekel A., Kolatt T. S., Kravtsov A. V., Klypin A. A., Porciani C., Primack J. R., 2001, *ApJ*, 555, 240
- Burkert A., et al., 2016, *ApJ*, 826, 214
- Butler K. M., Obreschkow D., Oh S.-H., 2017, *ApJ*, 834, L4
- Chabrier G., 2003, *ApJ*, 586, L133
- Chowdhury A., Chengalur J. N., 2017, *MNRAS*, 467, 3856
- Cortese L., et al., 2016, *MNRAS*, 463, 170
- Dalcanton J. J., Spergel D. N., Summers F. J., 1997, *ApJ*, 482, 659
- Di Teodoro E. M., Fraternali F., 2015, *MNRAS*, 451, 3021
- Dutton A. A., van den Bosch F. C., 2012, *MNRAS*, 421, 608
- Efstathiou G., Jones B. J. T., 1979, *MNRAS*, 186, 133
- El-Badry K., et al., 2018, *MNRAS*, 473, 1930
- Fall S. M., 1983, *IAUS*, 100, 391
- Fall S. M., Romanowsky A. J., 2013, *ApJ*, 769, L26
- Foreman-Mackey D., Hogg D. W., Lang D., Goodman J., 2013, *PASP*, 125, 306
- Genel S., Fall S. M., Hernquist L., Vogelsberger M., Snyder G. F., Rodriguez-Gomez V., Sijacki D., Springel V., 2015, *ApJ*, 804, L40
- Harrison C. M., et al., 2017, *MNRAS*, 467, 1965
- Iorio G., Fraternali F., Nipoti C., Di Teodoro E., Read J. I., Battaglia G., 2017, *MNRAS*, 466, 4159
- Kassin S. A., Devriendt J., Fall S. M., de Jong R. S., Allgood B., Primack J. R., 2012, *MNRAS*, 424, 502
- Knebe A., et al., 2015, *MNRAS*, 451, 4029
- Lelli F., McGaugh S. S., Schombert J. M., 2016a, *ApJ*, 816, L14
- Lelli F., McGaugh S. S., Schombert J. M., 2016b, *AJ*, 152, 157
- Lelli F., McGaugh S. S., Schombert J. M., Pawlowski M. S., 2017, *ApJ*, 836, 152
- Martinsson T. P. K., Verheijen M. A. W., Westfall K. B., Bershady M. A., Schechtman-Rook A., Andersen D. R., Swaters R. A., 2013, *A&A*, 557, A130
- McGaugh S. S., Schombert J. M., 2014, *AJ*, 148, 77
- Mitchell P. D., et al., 2018, *MNRAS*, 474, 492
- Mo H. J., Mao S., White S. D. M., 1998, *MNRAS*, 295, 319
- Navarro J. F., Frenk C. S., White S. D. M., 1996, *ApJ*, 462, 563
- Navarro J. F., Steinmetz M., 2000, *ApJ*, 538, 477
- Obreja A., Stinson G. S., Dutton A. A., Macciò A. V., Wang L., Kang X., 2016, *MNRAS*, 459, 467
- Obreschkow D., Glazebrook K., 2014, *ApJ*, 784, 26
- Peebles P. J. E., 1969, *ApJ*, 155, 393
- Ponomareva A. A., Verheijen M. A. W., Papastergis E., Bosma A., Peletier R. F., 2018, *MNRAS*, 474, 4366
- Posti L., Pezzulli G., Fraternali F., Di Teodoro E. M., 2018, *MNRAS*, 475, 232
- Planck Collaboration, Ade P. A. R., Aghanim N., et al. 2016, *A&A*, 594, A13
- Rodríguez-Puebla A., Avila-Reese V., Yang X., Foucaud S., Drory N., Jing Y. P., 2015, *ApJ*, 799, 130
- Romanowsky A. J., Fall S. M., 2012, *ApJS*, 203, 17
- Shi J., Lapi A., Mancuso C., Wang H., Danese L., 2017, *ApJ*, 843, 105
- Stevens A. R. H., Croton D. J., Mutch S. J., 2016, *MNRAS*, 461, 859
- Teklu A. F., Remus R.-S., Dolag K., Beck A. M., Burkert A., Schmidt A. S., Schulze F., Steinborn L. K., 2015, *ApJ*, 812, 29
- van den Bosch F. C., 1998, *ApJ*, 507, 601
- van den Bosch F. C., Burkert A., Swaters, R. A. 2001, *MNRAS*, 326, 1205
- Verheijen M. A. W., 2001, *ApJ*, 563, 694
- Zavala J., et al., 2016, *MNRAS*, 460, 4466

Appendix A: Asymmetric drift correction

The circular velocity V_c is equal to the sum in quadrature of the stellar rotation velocity $V_{*,\text{rot}}$ and the asymmetric drift velocity V_{AD} , i.e. $V_c^2 = V_{*,\text{rot}}^2 + V_{\text{AD}}^2$. We use the (inclination-corrected) HI observed rotation curve to trace V_c at each radius. Then, following the findings of the DiskMass Survey on a sample of 30 well-studied face-on nearby spirals (Martinsson et al. 2013), we assume the vertical stellar velocity dispersion to vary exponentially with radius $\sigma_z = \sigma_{0,z} \exp(-R/2R_d)$, where R_d is the disc scale length measured at $3.6 \mu\text{m}$. The normalisation $\sigma_{0,z}$ is found to be a function of the galaxy's central surface brightness μ_0 at $3.6 \mu\text{m}$: $\sigma_{z,0} \approx 20 \text{ km/s}$ for $\mu_0 \lesssim 20 \text{ mag/arcsec}^2$ and $\sigma_{z,0} \approx 70 \text{ km/s}$ for $\mu_0 \sim 16 \text{ mag/arcsec}^2$ (see Martinsson et al. 2013).

By further assuming that the disc scale height is constant with radius and that the system is isotropic, $\sigma_R = \sigma_z$, we can write the asymmetric drift velocity as (e.g. Binney & Tremaine 2008, §4.8.2)

$$V_{\text{AD}}^2 = \sigma_{0,z}^2 \frac{3R}{2R_d} e^{-R/2R_d}. \quad (\text{A.1})$$

In this Letter we use Eq. A.1 to correct for asymmetric drift. In general, this introduces just a small correction, of less than 5%, to the estimate of the specific angular momentum. We have also considered i) the anisotropic case $\sigma_z^2 = \sigma_R^2/2$ and ii) the extreme case of a uniform vertical dispersion $\sigma_z = \sigma_{0,z}$ throughout the galaxy and found in both cases small differences (less than 10%) in the derived specific angular momenta.